Nucleic Acids Research Advance Access published July 4, 2016

*Nucleic Acids Research, 2016* **1**
*doi: 10.1093/nar/gkw611*

# RecA stimulates AlkB-mediated direct repair of DNA adducts

**Gururaj Shivange, Mohan Monisha, Richa Nigam, Naveena Kodipelli and Roy Anindya***

Department of Biotechnology, Indian Institute of Technology Hyderabad, Kandi, 502285 Hyderabad, Telangana, India

Received January 9, 2016; Revised June 27, 2016; Accepted June 28, 2016

## ABSTRACT

**The *Escherichia coli* AlkB protein is a 2-oxoglutarate/Fe(II)-dependent demethylase that repairs alkylated single stranded and double stranded DNA. Immunoaffinity chromatography coupled with mass spectrometry identified RecA, a key factor in homologous recombination, as an AlkB-associated protein. The interaction between AlkB and RecA was validated by yeast two-hybrid assay; size-exclusion chromatography and standard pull down experiment and was shown to be direct and mediated by the N-terminal domain of RecA. RecA binding results AlkB–RecA heterodimer formation and RecA–AlkB repairs alkylated DNA with higher efficiency than AlkB alone.**

## INTRODUCTION

DNA damaging alkylating agents are present abundantly in the environment and also produced endogenously. The majority of the DNA adducts caused by such alkylating agents would be in double-stranded DNA. However, single-strand-specific lesions can arise when DNA double helix is temporarily unwound during replication or recombination. The N1 position of purines and N3 of pyrimidines, which are normally protected from alkylation by base pairing in duplex DNA, can be specifically alkylated in single-stranded DNA (ssDNA). For example, simple methylating agents, such as methyl methane sulfonate (MMS), generates N1-methyladenine (N1-meA) and N3-methylcytosine (N3-meC) on ssDNA (1). Another example is, oxidative stress-induced endogenous lipid peroxidation, which generates aldehydes that reacts with DNA to form etheno(ϵ)-adducts (2): among these, 1,N6-ethenoadenine (ϵA) and 3,N4-ethenocytosine (ϵC) are found predominantly in ssDNA (3). These alkylated bases are unable to form normal Watson–Crick base pairs and therefore, block DNA replication and resulting in cytotoxicity (4).

While there are multiple mechanisms dedicated to the repair of DNA alkylation damage from the double-stranded DNA, a single class of DNA repair enzyme belonging to the Fe(II)/2-oxoglutarate-dependent dioxygenase family removes alkylated base lesions specifically from ssDNA. This enzyme is known as alkylation repair protein-B (AlkB) in *Escherichia coli* and directly repairs N1-meA and N3-meC (5,6). Highlighting its critical function, homologs of AlkB have been identified across species ranging from bacteria to human (7). AlkB catalyzes oxidative dealkylation in a reaction requiring oxygen, non-heme iron ($Fe^{II}$) as cofactors, 2OG as a co-substrate resulting in the formation of succinate and $CO_2$. When AlkB repairs N1-meA or N3-meC, the methyl group is removed as formaldehyde (8); whereas, its repair of exocyclic etheno adducts ϵA and ϵC removes etheno group as glyoxal (9).

It has been reported that AlkB prefers damaged ssDNA over undamaged ssDNA as a substrate (10) and AlkB identifies alkylated base lesions by scanning the genome (11). To gain a more complete understanding of the mechanism of recruitment of AlkB, we purified AlkB and performed a targeted proteomic analysis of proteins co-purified with AlkB protein using mass spectrometry. Here, we report an interaction between AlkB and the recombination repair factor RecA. RecA protein is found in all organism and essential for genetic recombination and recombinational DNA repair (12,13). The *E. coli* RecA protein is a 352 amino acid polypeptide and essential for recombination. The structure of RecA protein reveals a large core domain, and two smaller domains at the N- and C-termini (14–16). In the active RecA filament, adenosine triphosphate (ATP) is bound at the subunit–subunit interface (17). RecA protein binds to the single-stranded DNA with one RecA monomer for every three bases of DNA and forms nucleoprotein filament accompanied by ATP hydrolysis. This RecA filaments promote alignment with a homologous duplex DNA, strand exchange and branch migration (18). Beside nucleoprotein filament formation, RecA also has co-protease activity, which facilitates the autocatalytic cleavage of the LexA repressor. LexA is the repressor of many DNA damage-inducible genes, including *recA* and cleavage of LexA repressor promote induction of many *lexA* regulated genes. This response to DNA damage is known as SOS response (19). RecA also directly facilitate replicative bypass of DNA lesions by associating with DNA polymerase-V (pol-V) during SOS response (20).

In this report, we provide biochemical evidence that purified AlkB and RecA forms stable complex whereby RecA

*To whom correspondence should be addressed. Tel: +91 40 2301 6083; Fax: +91 40 2301 6032; Email: anindya@iith.ac.in

enhances AlkB-catalyzed repair of methyl ssDNA adducts. To our knowledge, the only other functionally important interaction of RecA that has been reported so far is with DNA pol-V (21).

## MATERIALS AND METHODS

### Plasmid constructs

Cloning was accomplished using standard techniques and confirmed by sequencing. For construction of GST fusion proteins, *E. coli recA* and *alkB* genes were PCR amplified from genomic DNA using appropriate primers and cloned into pGex6p1 (GE Healthcare), using BamHI and XhoI restriction enzymes. For construction of N-terminal His-tag fusion proteins, *E. coli* AlkB, RecA and Δ33RecA were cloned into pET-28a (Novagen) using BamHI and XhoI restriction enzymes.

### Purification of AlkB associated proteins

*Escherichia coli* BL21-CodonPlus(DE3)-RIL (Stratagene) cells carrying pET-28a-AlkB plasmid or pET-28a vector were induced for protein expression by 1 mM isopropyl β-D-thiogalactopyranoside (IPTG). About 4 h after induction, cells were harvested, disrupted by sonication and total extracts were prepared in extraction buffer (20 mM Tris, pH 8.0, 500 mM NaCl, 10 mM imidazole and protease inhibitors) Ni-NTA-agarose beads (Qiagen) (≈400 μl of packed beads per litre of starting culture) were added to the extract and incubated for 4 h at 4°C. After binding of the protein complexes, beads were washed extensively with the washing buffer (20 mM Tris, pH 8.0, 500 mM NaCl, 50 mM imidazole and cOmplete-mini protease inhibitors (Roche, GmbH)). Finally, purified protein complexes were eluted in elution buffer (20 mM Tris, pH 8.0, 150 mM NaCl, 250 mM imidazole) and protease inhibitors. Eluates were resolved in 4–12% bis-Tris gradient PAGE and the protein bands were excised for mass spectrometry.

### Mass spectrometric analysis

Sample peptides were generated by the *in situ* tryptic digestion of the gel bands. LC/MS/MS analysis of the peptides was performed by a Bruker Daltonics-UltraflexTMIII mass spectrometer. The resulting mass spectrometry data were then searched against the UniProt protein database by using the PLGS platform.

### Purification of recombinant proteins

Plasmids were transformed into the *E. coli* strain BL21-CodonPlus(DE3)-RIL (Stratagene), and protein expression was induced by the addition of 1 mM IPTG. Cells were disrupted by sonication. GST tagged proteins were purified using affinity purification with glutathione–Sepharose 4B medium (GE Healthcare), and His-tagged proteins were purified using Ni-NTA agarose (Qiagen). All the proteins were finally dialyzed against 10 mM Tris–HCl pH 7.4, 100 mM NaCl and 5% glycerol. Proteins were analyzed by 12% sodium dodecyl sulphate-polyacrylamide gel electrophoresis (SDS-PAGE) and subsequently by Coomassie Brilliant Blue staining and concentrations were determined by Bradford assays (Bio-Rad).

### CD spectroscopy

The circular dichroism (CD) experiments were conducted on a JASCO J-1500 instrument. A 1 mm path length quartz cell was used with 20 μM RecA or Δ33RecA. Spectra were obtained at room temperature in buffer containing 10 mM Tris–HCl, pH 7.4, 50 mM NaCl.

### *In vitro* binding assay

For GST pull-down experiments, 120 μg of GST-tagged proteins bound to 50 μl glutathione sepharose beads (Thermo Scientific) was incubated with ∼175 μg of free His-tagged proteins in 500 μl binding buffer containing 10 mM Tris–HCl pH 7.4, 100 mM NaCl and 5% glycerol at room temperature for 2 h. Protein complexes were then pulled down with glutathione-sepharose beads. After removing non-specific proteins by washing the beads with 500 μl phosphate buffered saline four times, 10 μl was analyzed by 12% SDS-PAGE and subjected to western blot analysis using an anti-6xHis antibody (1:1000; GE healthcare).

### Yeast two-hybrid analysis

The pACT2-RecA, pACT2-RecA-NTD, pACT2-Δ33RecA (activation domain) plasmid was cotransformed with pGBKT7-AlkB (binding domain) plasmid into yeast strain pJ69-4A to generate strain J69RA1 (pACT2-RecA + pGBKT7-AlkB), J69RA2 (pACT2-RecA-NTD + pGBKT7-AlkB) and J69RA3 (pACT2–Δ33RecA + pGBKT7-AlkB). The transformants were plated onto synthetic defined (SD) -Leu -Trp dropout plates and incubated at 30°C for 2–3 days. The double dropout plates allow the growth of yeast cells with the two fusion plasmids. The transformants were further spotting onto SD -Leu -Trp -His plates, which were incubated at 30°C for 3–5 days to examine the growth. The interaction of the two fusion proteins activates the reporter genes, resulting in the growth of yeast cells on the triple dropout plates. The β-galactosidase (β-gal) activity was measured according to the Yeast Protocols Handbook (Clontech). In brief, yeast cells grown in SD −Leu −Trp dropout medium for 48 h at 30°C were transferred onto filter paper and the cells were lysed in liquid nitrogen for 1 min. Filter disc was then kept on another sterile filter paper, pre-soaked in 5 ml Z buffer (60 mM $Na_2HPO_4$, 40 mM $NaH_2PO_4$, 10 mM KCl, 1 mM $MgSO_4$, 40mM β-mercaptoethanol) containing 8 mg/ml X-gal. Appearance of blue color was monitored for 30 min to 10 h.

### Analysis of RecA–AlkB interaction by size exclusion chromatography

Samples of purified recombinant proteins were applied to Superose-12 (GE Healthcare) gel filtration column and analyzed using an AKTA Prime FPLC system (GE Healthcare). For analysis of RecA–AlkB complex, 0.5 mg (35 μM) of AlkB was mixed with 0.735 mg (35 μM) of RecA in 0.5 ml buffer containing 25 mM NaCl and 20 mM HEPES, pH 7.0

or 20 mM Tris–HCl, pH 8.0 or 9.0. *E. coli* RecA (EcRecA) was purchased from New England Biolabs (M0249L). For the analysis of EcRecA, 0.5 mg (35 μM) of AlkB was mixed with 0.735 mg (35 μM) of RecA in 0.5 ml buffer containing 100 mM NaCl and 20 mM HEPES, pH 7.0 or 20 mM Tris–HCl, pH 8.0. For the SEC analysis of RecA titration 20 μM of AlkB was mixed with, 20, 40, 80, 160 μM RecA protein. For AlkB titration 20 μM of RecA was mixed with, 20, 40, 80 μM AlkB protein. The samples were analyzed with flow rate of 0.3 ml/min and 0.5 ml fractions were collected.

### Docking analysis

The three-dimensional structure coordinates of the two proteins namely AlkB (3KHC) and RecA (2REB) were retrieved from Protein Data Bank. The molecular docking of AlkB with RecA was performed using two docking tools namely ZDOCK and Cluspro. ZDOCK is a rigid-body protein–protein docking tool uses that employs the fast fourier transform algorithm to perform the global docking analysis (22). This docking program involves a combination of both shape complementarity and electrostatics terms for the scoring of the docked poses. Cluspro is another fully automated rigid-body docking tool that ranks the docked conformations based on the clustering properties (23). This docking algorithms first evaluates structures with promising surface complementarities and later, docks the structures that have the good desolvation and electrostatic energies (24). The top 20 docked complexes of RecA–AlkB obtained were shortlisted based on the two parameters namely the atomic contact energy and geometric shape complementarity score. The docked complexes were further subjected to FireDock for the post-energy minimization. Finally, the docked output complexes were analyzed to identify the best possible conformations and residues of AlkB interacting with RecA monomer using Discovery Studio Visualizer 2.5 and PyMOL Molecular Graphics System, Version 1.3, Schrodinger, LLC.

### Demethylation assay

AlkB-mediated demethylation was measured by repair of N3-meC present in 40-mer N3-me oligo-dC. SN2 alkylating agents such as MMS reacts with N3 position of cytosine to generate N3-meC. We modified 40-mer oligo-dC to N3-me oligo-dC by MMS treatment and used this as AlkB substrate in the repair assay. In brief, 40 μg of chemically synthesized 40-mer oligo-dC (Imperial Life science) was treated with 5% (v/v) (0.59 M) MMS (Sigma, 129 925) in a final volume of 500 μl in presence of 200 mM $K_2HPO_4$ for 14 h at room temperature. The methylated DNA was not purified directly by using ethanol precipitation as it resulted poor yield. Therefore, excess MMS was removed by dialysis against TE buffer (10 mM Tris. pH 8.0, 1 mM ethylenediaminetetraacetic acid) using Spectra/Por dialysis membrane (MWCO: 3500). The damaged DNA was precipitated by adding 0.3 M sodium acetate pH 5.5 and two volume of ice-cold ethanol. The precipitated methylated DNA was washed with 70% ethanol and finally dissolved in water. After calculating extent of damage (supplemental information materials and methods) 40-mer N3-me oligo-dC was used for demethylation assay. Repair reactions (50 μl) were carried out at 37°C for 1 h in the presence of 1 μM AlkB and 0.5 μg (1 μM) 40-mer N3-me oligo-dC in reaction buffer containing 20 mM Tris–HCl pH 8.0, 200 μM 2OG, 2 mM L-Ascorbate, 20 μM $Fe(NH_4)_2(SO_4)_2$. The released formaldehyde was directly quantified from the reaction mixture.

### Formaldehyde detection with acetoacetanilide

Formaldehyde detection with acetoacetanilide is based on reaction of formaldehyde with acetoacetanilide and ammonia which form an enamine-type intermediate. This intermediate undergoes cyclodehydration to generate highly fluorescent dihydropyridine derivative, having maximum excitation at 365 nm and maximum emission at 465 nm. Formaldehyde standard curve was prepared by selecting a range of pure formaldehyde concentrations from 2 to 20 μM. To detect formaldehyde, a 50 μl sample containing pure formaldehyde or demethylation repair reaction product was mixed with 40 μl of 5 M ammonium acetate and 10 μl of 0.5 M acetoacetanilide to make the final volume 100 μl. The fluorescent compound was allowed to develop at room temperature for 15 min and then entire reaction mixture was transferred to 96-well microplate and analyzed using a SpectraMax M5e (Molecular Devices) multimode reader setting the excitation wavelength at 365 nm and emission wavelength at 465 nm.

### The effect of RecA on AlkB demethylation activity

The effect of RecA nucleoprotein filament on demethylation activity of RecA was determined by incubating 0.25 μM RecA–AlkB complex and 1 μM 40-mer N3-me oligo-dC in the presence of 20 mM Tris–HCl (pH 8.0) in a final volume of 50 μl. The efficiency of repair was monitored by detecting the released formaldehyde. To determine the amount of RecA protein required to achieve maximum stimulation of AlkB activity, increasing concentration of purified his-tag RecA protein (0.87–28 μM) were incubated with 1 μM of 40-mer N3-me oligo-dC for 15 min at 37°C in a total volume of 50 μl. All the repair reactions were carried out at 37°C for 1 h. A total of 40-mer undamaged oligo-dC was incubated with AlkB as control. To monitor the effect of Mg2+ and ATP, 1 mM of $MgCl_2$ and 300 μM of ATP-γ-S was added with 7 μM RecA, 1 μM AlkB and 1 μM 40-mer N3-me oligo-dC in a total reaction volume of 100 μl. Repair reaction was also carried out with bovine serum albumin (BSA) (7 μM) instead of RecA. To determine the effect of undamaged ssDNA on repair, 10 μM of 40-mer undamaged oligo-dC was added with 7 μM RecA, 1 μM AlkB and 1 μM 40-mer N3-me oligo-dC in a total reaction volume of 100 μl. DNA repair with mutant AlkB were carried out by mixing 7 μM RecA, 1 μM of AlkB with H131A and H133A mutation and 1 μM 40-mer N3-me oligo-dC in a total reaction volume of 100 μl.

## RESULTS AND DISCUSSION

### RecA is an AlkB-associated protein

We initiated our study with a thorough proteomic analysis of the AlkB. To find out the AlkB interacting proteins, we over-expressed His-tagged AlkB in *E.coli* BL21

cells and purified it under stringent condition using Ni-NTA agarose. Parallel control purification from the same amount of uninduced cell extract was performed to evaluate the non-specific protein pull down (Figure 1A). The low background in our experimental system encouraged us to identify the proteins that were co-eluted with the AlkB. Protein bands were excised and mass-spectrometric (MS) peptide identification was performed. Expectedly, AlkB was identified as the major protein in the sample. Identities of all the proteins are described in the Supplementary Table S1. By removing proteins that were also identified in the control pull-down, we identified AlkB-associated factors. A number of these factors, such as the β and δ-subunit of DNA polymerase-III, DnaB and RecG helicase, are known to be involved in DNA replication and repair, providing further evidence that the experimental strategy was robust (Figure 1B). RecA, a factor essential for homologous genetic recombination and repairing damaged chromosomal DNA by mediating homologous recombination, was also identified as a novel AlkB-interacting protein. We focused our efforts on RecA, since it has not previously been described as having a role in AlkB-mediated DNA repair.

To determine whether the RecA–AlkB interaction was direct or mediated via secondary interactions with other proteins, we conducted GST-pull down assays with bacterially expressed GST-RecA and His-AlkB (Figure 1C). Using GST-RecA protein as 'bait', His-tag AlkB was captured as detected by immunoblot analysis using anti-His antibody (Figure 1D, upper panel, lane 2). This interaction was highly robust, as AlkB was detectable even when the membrane was stained with Ponceau-S, which is much less sensitive than Western blotting (Figure 1D, lower panel, compare lane 2 with lane 1). However, no AlkB was pull down when GST protein was used as 'bait' (Figure 1D, upper panel, lane 3). These results indicate that RecA interacts directly with AlkB and also suggest that each protein probably has binding site for the other.

To further validate the RecA–AlkB interaction, we used a yeast two-hybrid approach. *recA* and *alkB* genes were cloned into vectors pGBKT7 (TRP1 marker) and pACT2 (LEU2 marker). pACT2-RecA and pGBKT7-AlkB express fusion proteins with Gal4 DNA binding and activation domains, respectively. The yeast two-hybrid reporter strain PJ69-4A contains ADE2, HIS3, *lacZ* reporter genes that are expressed only when a functional Gal4 protein is formed by an interaction between the DNA binding domain and activation domain. PJ69-4A cells carrying plasmid pair pACT2-RecA/pGBKT7-AlkB grew on media lacking histidine, tryptophan, and leucine, and showed a blue color on media supplemented with X-gal, indicating both *lacZ* and HIS3 reporter gene expression in these cells (Figure 1E). Taken together, the results of the two-hybrid experiment support the conclusion that the two proteins directly bind each other.

### RecA forms stable complex with AlkB

The results enumerated above clearly establish RecA–AlkB interaction. To examine if RecA forms stable complex with AlkB or they interact transiently, we analyzed their interaction by size exclusion chromatography (SEC). First, recombinant RecA and AlkB purified from *E. coli* were applied separately to a Superose-12 SEC column equilibrated with 25 mM NaCl and 20 mM Tris–HCl, pH 8.0. Eluted fractions were applied to SDS-PAGE to detect and identify the protein contents. SEC analysis of RecA (35 μM) showed that RecA protein was eluted predominantly near the void volume of the column (8 ml), although small fractions of the proteins were also eluted at larger volumes (Figure 1F). This is probably due to existence of RecA as various oligomers in equilibrium. In the absence of DNA, RecA protein can self assemble into a variety of multimeric forms, including rings, rods and highly aggregated structures and it has been shown that these aggregation states are in reversible equilibrium depending on the pH of the buffer, salt conditions and protein concentrations (25). AlkB protein was found in a distinct peak at an elution volume of ∼14 ml, which corresponds to a molecular mass of ∼24 kDa (Figure 1F). This indicates that AlkB purified from *E. coli* exists as a monomer.

To elucidate characteristics of the AlkB–RecA protein complex, equal concentrations (35 μM) of the proteins were mixed and assessed by SEC. The highest concentrations of RecA and AlkB were eluted at 8 ml and 14 ml, respectively, indicating the individual proteins (Figure 1G). However, a moderate amount of both factors was detected in a fraction at ∼11 ml, suggesting the formation of a protein complex (Figure 1G, bottom panel). Interestingly, almost no AlkB protein was detected in the void fractions, suggesting that AlkB did not bind aggregated RecA (Figure 1G, bottom panel). To assess the stability of this putative RecA–AlkB complex, we subjected this fraction to another round of gel filtration. Both factors eluted reproducibly at 11 ml, suggesting that they form a stable complex in the experimental conditions (Figure 1H). Chromatogram of this complex closely overlapped with BSA suggesting a molecular weight of ∼63 kDa. SDS-PAGE analysis of the gel filtration fractions revealed approximately equal proportion of RecA and AlkB were present at the peak elution volume 11 ml (Figure 1H, bottom panel). We have observed that the key factor that affects the complex formation is pH. Stable RecA–AlkB complex was formed at pH 8.0 and pH 9.0 when His-tag RecA was used (Figure 2A). However, native *E. coli* RecA (without His-tag) formed complex with AlkB at pH 7.0 and at pH 8.0 or above no RecA–AlkB interaction was observed. This result suggests that N-terminal His-tag alters the RecA interaction with AlkB (Figure 2B). Longer incubation of RecA with AlkB did not result higher yield of RecA–lkB complex (Figure 2C). Similarly, the presence of ATP had no effect on RecA–AlkB complex formation (Figure 2D). These results led us to conclude that RecA binds to AlkB and RecA–AlkB may exist as stable heterodimer. Although we observed a 1:1 complex, the complex elutes as a minor species between the main RecA and AlkB peaks. RecA is known to form filaments on ssDNA in the presence of ATP and Mg2+; however, in the absence of ATP, RecA undergoes self-aggregation and only limited amount of RecA protein is present as free monomeric form which is available for binding to AlkB. This is probably the reason why a small fraction of RecA and AlkB protein forms complex. We hypothesized that presence of more RecA protein with respect to AlkB might provide more free monomeric

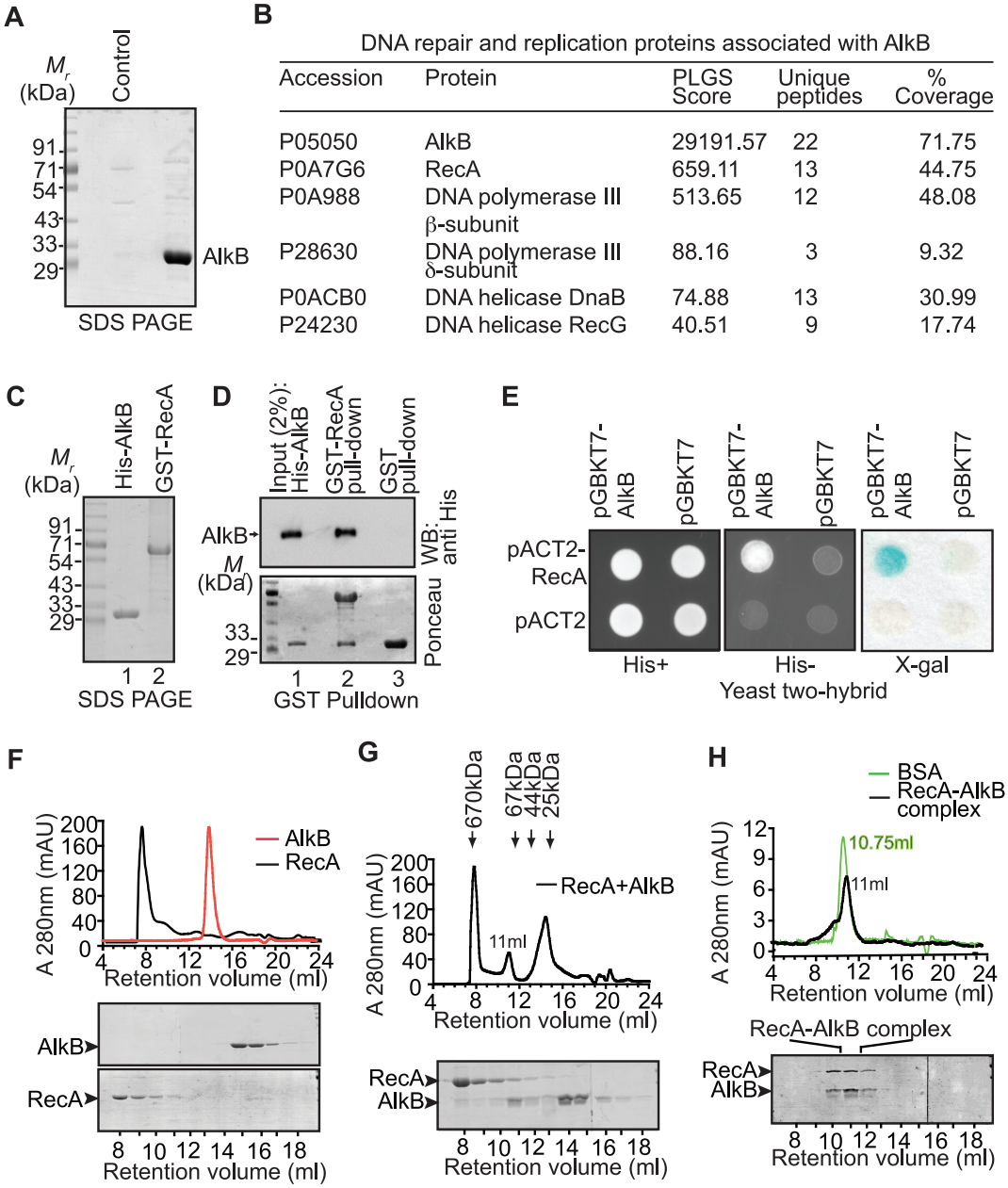


| Accession | Protein | PLGS Score | Unique peptides | % Coverage |
|---|---|---|---|---|
| P05050 | AlkB | 29191.57 | 22 | 71.75 |
| P0A7G6 | RecA | 659.11 | 13 | 44.75 |
| P0A988 | DNA polymerase III β-subunit | 513.65 | 12 | 48.08 |
| P28630 | DNA polymerase III δ-subunit | 88.16 | 3 | 9.32 |
| P0ACB0 | DNA helicase DnaB | 74.88 | 13 | 30.99 |
| P24230 | DNA helicase RecG | 40.51 | 9 | 17.74 |

**Figure 1.** Identification and confirmation of interaction of AlkB with RecA. (**A**) AlkB-associated proteins were analyzed by 10% sulphate-polyacrylamide gel electrophoresis (SDS-PAGE). (**B**) The identities of proteins involved in DNA repair or replication identified by LC/MS. Complete list of proteins are included in Supplementary Table S1. (**C**) Confirmation of the RecA–AlkB interaction by GST pull down experiment. SDS-PAGE analysis of purified His-tag AlkB and GST RecA. (**D**) His-tag AlkB and GST RecA bound to glutathione sepharose beads was mixed together and interacting proteins were pull down by glutathione sepharose. Top: inputs and pull downs were separated by SDS-PAGE and analyzed by western blot with anti-His antibody. Bottom: Ponceau-S staining. Note that in Ponceau-S stained blot, upper band in the lane 2 represent GST-RecA (from bead) and the lower band is pull down His-tag AlkB; the band in lane 3 represent GST (from bead) which moves at the same position as His-tag AlkB (**E**) AlkB interacts with RecA in the yeast two-hybrid system. Yeast cells carrying plasmid pACT2, pACT2-RecA, pGBKT7 and pGBKT7-AlkB were spotted on plates with appropriate media. Positive interactions are indicated by growth on media lacking histidine (middle) and the expression of β-galactosidase (β-gal) (right). (**F**) Analysis of RecA and AlkB by SEC. A total of 35 μM of RecA or AlkB present in 20 mM Tris–HCl, pH 8.0, 25 mM NaCl analyzed by Superose-12 FPLC column. RecA eluted as high molecular weight aggregate. AlkB eluted as monomer. (**G**) RecA and AlkB were mixed together in the same buffer (mentioned above) and analyzed by SEC. A new peak was observed at 11 ml, separate from RecA and AlkB peaks. (**H**) Purified of RecA–AlkB complex (63 kDa). Peak position of pure bovine serum albumin (BSA) corresponding to molecular weight 66 kDa is also seen in the chromatogram. An aliquot of each fraction obtained from SEC was analyzed by SDS-PAGE (F, G and H, bottom panels).

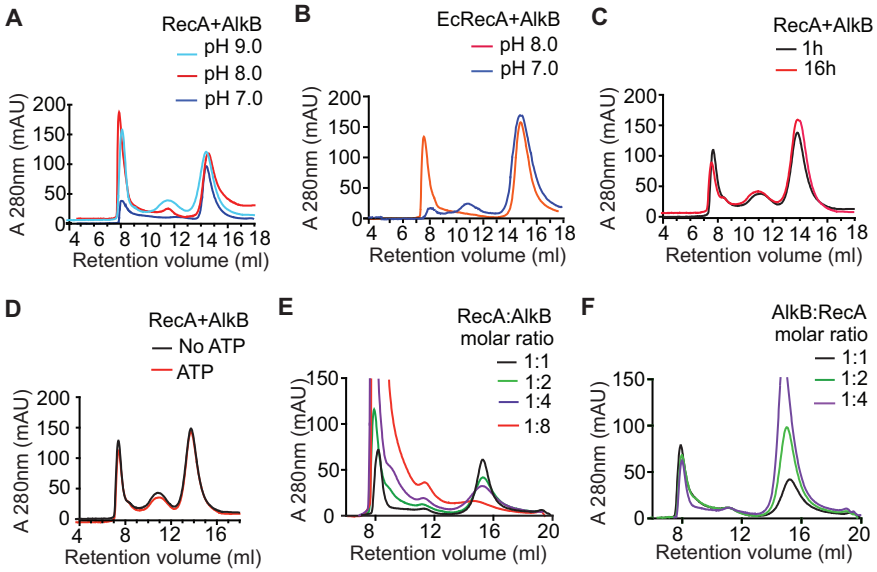


**Figure 2.** AlkB–RecA interaction. (**A**) SEC of His-tag RecA and AlkB at different pH. About 35 μM of RecA and AlkB were mixed together in 20 mM Tris–HCl, pH 7.0, 8.0 and 9.0, containing 25 mM NaCl. RecA–AlkB complex eluted as a peak at 11 ml. (**B**) SEC of *Escherichia coli* RecA (without his-tag) and AlkB at different pH. About 35 μM of RecA and AlkB were mixed together in 20 mM Tris–HCl, pH 7.0 and 8.0 containing 100 mM NaCl. RecA–AlkB complex eluted as a peak at 11 ml. (**C**) Effect of incubation time on formation of RecA–AlkB complex analyzed by SEC. About 35 μM of RecA and AlkB were mixed together in 20 mM Tris–HCl, pH 9.0, 25 mM NaCl, for 1 or 16 h. (**D**) Effect of ATP on RecA–AlkB complex formation was also monitored by SEC. About 35 μM of RecA and AlkB was mixed with 20 mM Tris–HCl, pH 9.0, 25 mM NaCl, 1 mM ATP and 10 mM $MgCl_2$. RecA–AlkB complex eluted as a peak at 11 ml. (**E**) SEC analysis of RecA titration. AlkB (20 μM) was mixed with 20 (1:1), 40(1:2), 80(1:4), 160 μM(1:8) RecA protein in 20 mM Tris–HCl, pH 9.0. (**F**) SEC analysis of AlkB titration. About 20 μM of RecA was mixed with 20(1:1), 40(1:2), 80(1:4) μM AlkB protein in 20 mM Tris–HCl, pH 9.0.

RecA fraction and facilitate AlkB–RecA complex formation. Indeed, when RecA protein is present in the 8-fold molar excess compared to AlkB, almost all of AlkB protein forms AlkB–RecA dimeric complex while the majority of the RecA protein remained as aggregate (Figure 2E). In contrast, when we gradually increased the AlkB concentration with fixed concentration of RecA, amount of AlkB–RecA complex did not change (Figure 2F). These results suggest RecA–AlkB heterodimer formation depends on free monomeric RecA.

### Amino-terminal domain of RecA is involved in interaction with AlkB

In light of our results demonstrating physical interaction between AlkB and RecA, we wanted to identify putative sites of the interaction of RecA with AlkB. For this we turned to *in silico* docking approach to identify potential binding sites that may be present on the surface of the two proteins. The potential binding regions of AlkB with RecA protein were predicted using two docking approaches, namely, ClusPro and ZDOCK. The top clustering outputs from each of these programs were considered for further analysis. We found that the best shape complementarities, lowest desolvation and electrostatic energies were all consistently found when AlkB interacted with the amino-terminal domain (NTD) of RecA (Figure 3A). The Global Energy value and Attractive van der Waals energy of the docked complex after Firedock analysis were −4.75 Kcal/mol and −23.45 Kcal/mol respectively. Analysis with ClusPro docking tool gave the lowest clustering scores of −722.8 with RecA and AlkB. The AlkB protein adopts an energetically favorable conformation and interacts without any stearic hindrance with RecA protein. It was observed that the residues 1–33 which constitutes the NTD of the RecA protein was majorly interacting with AlkB, although few residues from core region of RecA protein were also showing interactions (Figure 3B). When ZDock was used, we observed Lys6, Ile26 and Ile29 of RecA NTD interacting with AlkB, albeit identities of the corresponding amino acid residues of AlkB were different (Supplementary Figure S4A and B). The non-covalent interactions of the RecA and AlkB were monitored using protein-ligand interaction analysis tool from Schrodinger, LLC. It was noted that both ClusPro and ZDock analysis predicted different AlkB residues interacting with the same RecA NTD amino acid residues (Supplementary Figure S4). For example, ClusPro analysis showed interaction of Lys6, Ile26 and Leu29 of RecA with Tyr109, Phe25 and Trp11 residues of AlkB; whereas, ZDock analysis showed interaction of Lys6, Ile26 and Leu29 of RecA with Asp39, Ile34 and Ala29 residues of AlkB (Supplementary Figure S4). Nevertheless, the molecular docking simulations strongly suggested that the NTD of RecA might provide a stable interaction platform with AlkB.

To test whether N-terminal of RecA is indeed involved in interaction, a truncated RecA protein lacking the N-terminal 33 amino acid residues (Δ33RecA) was generated (Figure 3C). To examine whether elimination 33 amino acids of NTD affects proper folding, CD analysis was performed. As shown in Figure 3D, CD spectra of RecA and Δ33RecA were suggestive of the typical helical conforma-

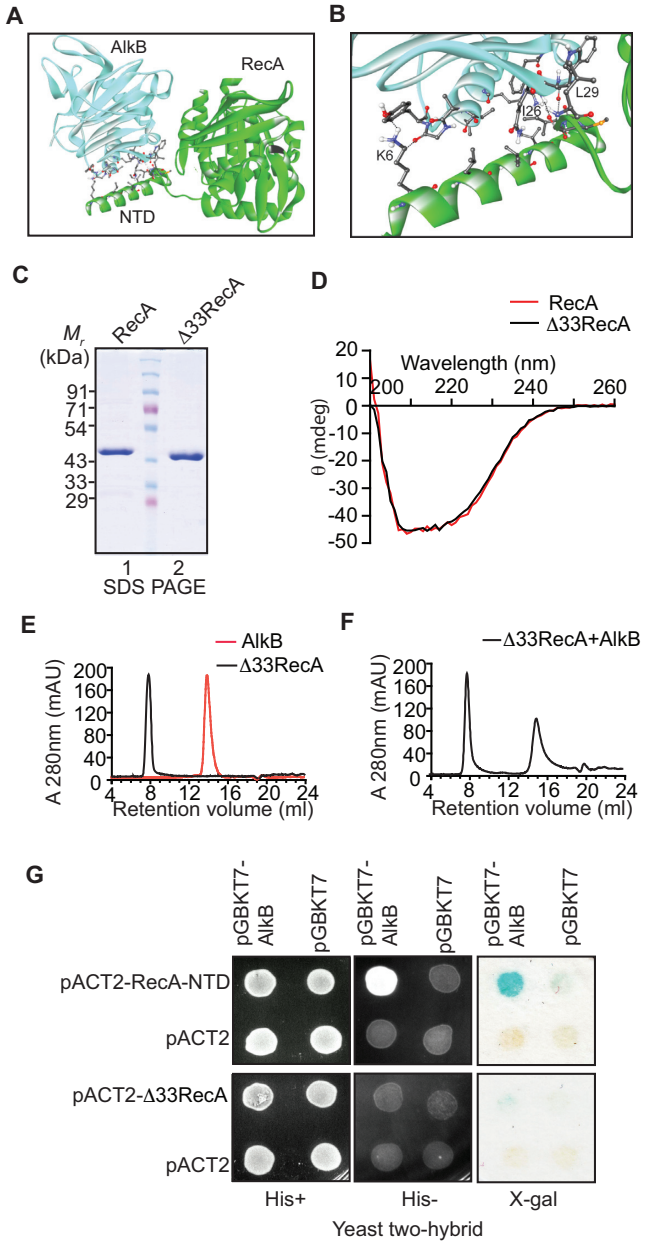


**Figure 3.** N-terminal domain of RecA is important for interaction with AlkB. (**A**) Docking analysis of AlkB protein and RecA protein. The coordinates of AlkB (3KHC) and monomeric RecA (2REB) were submitted to the ClusPro protein–protein docking server. AlkB is colored in cyan and monomeric RecA is in green, with the interacting residues are shown in sticks. (**B**) Enlarged view of the interacting residues of AlkB and RecA. (**C**) SDS-PAGE analysis of purified recombinant His-tag RecA and His-tag Δ33RecA; (**D**) Circular dichroism (CD) spectroscopy of RecA (red trace) and Δ33RecA (black trace). Spectra were obtained at room temperature using RecA or Δ33RecA (20 μM) in buffer containing 10 mM Tris–HCl, pH 7.4, 50 mM NaCl. (**E**) SEC of purified Δ33RecA and AlkB (35 μM). (**F**) AlkB and Δ33RecA (35 μM) were mixed in 20 mM Tris–HCl, pH 8.0 containing 25 mM NaCl. Δ33RecA eluted as high molecular weight aggregate and AlkB eluted as monomer. (**G**) AlkB interacts with N-terminal 33 amino acid residues of RecA (RecA-NTD) in the yeast two-hybrid system. Yeast cells carrying plasmid pACT2, pACT2-RecA-NTD, pACT2-Δ33RecA, pGBKT7 and pGBKT7-AlkB were spotted on plates with appropriate media. Positive interactions are indicated by growth on media lacking histidine (middle) and the expression of β-gal (right).

tion. Previous studies have shown that mutation of the RecA N-terminal domain affects filament formation on ssDNA (26). We analyzed Δ33RecA protein by SEC and found that, like the canonical RecA, Δ33RecA eluted predominantly near the void volume of the column, suggesting the formation of large aggregates (Figure 3E). To investigate whether the N-terminal domain of RecA was involved in AlkB interaction, AlkB was mixed with Δ33RecA exactly like RecA and incubated for 16 h. As shown in Figure 3F, no peak corresponding to a RecA–AlkB protein complex was observed during SEC analysis, which was further supported by SDS-PAGE (not shown). Our findings indicate that the NTD of RecA is specifically involved in interaction with AlkB.

To further validate the role of RecA-NTD in AlkB interaction, we used yeast two-hybrid analysis. RecA-NTD and Δ33RecA were cloned into pACT2 vector (*LEU2* marker). PJ69-4A cells carrying plasmid pair pACT2-Δ33RecA/pGBKT7-AlkB failed to grow on media lacking histidine, tryptophan, and leucine, and did not show blue color on media supplemented with X-gal, indicating that neither of *lacZ* and *HIS3* reporter gene were expressing in these cells (Figure 3G). However, PJ69-4A cells carrying plasmid pair pACT2-RecA-NTD/pGBKT7-AlkB grew on media lacking histidine, tryptophan, and leucine, and also showed a blue color on media supplemented with X-gal, indicating both *lacZ* and *HIS3* reporter gene expression in these cells (Figure 3G). These results strongly suggest that NTD of RecA can interact with AlkB. Taken together, the results of SEC analysis and two-hybrid experiment corroborated the prediction from the docking analysis that NTD of RecA is specifically involved in interaction with AlkB (Figure 3A and B).

### RecA stimulates AlkB-catalyzed oxidative demethylation

An essential function of AlkB in DNA repair is its capacity to oxidatively demethylate methyl base lesions particularly present in ssDNA. Having established that purified RecA interacts with AlkB, we were keen to know if RecA–AlkB complex is functionally important and RecA binding could enhance AlkB activity. We used single-stranded 3-methyl cytosine substrate which was prepared by treating 40-mer oligonucleotide with SN2 alkylating agent MMS. DNA repair was assayed by measuring formaldehyde release as result of removal of methyl-adducts. Formaldehyde was detected by adding acetoacetanilide and ammonia directly to the reaction mix to form fluorescent compound with peak emission of 465 nm (27) (Supplementary Figure S1A). Concentration of released formaldehyde was determined from the formaldehyde standard curve (Supplementary Figure S1B and C). To determine extent of methylation, 40-mer N3-me oligo-dC and undamaged oligo-dC were completely digested with exonuclease-1, exonuclease-T and dephosphorylated by alkaline phosphatase. Resulting nucleosides were separated by HPLC. As shown in Supplementary Figure S2A and B, comparison of digestion profile of 40-mer N3-me oligo-dC and undamaged oligo-dC revealed that 47.7% of the residues were modified. Based on this estimation the concentration of 150 ng/μl of 40-mer N3-meC was estimated to be 12.7 μM. We were acutely

aware that the distribution of 3-methyl cytosine might be influenced by the precise concentration of DNA in the *in vitro* methylation reaction during substrate preparation. Strenuous efforts were therefore made to perform all key assays in parallel and to ensure that the results obtained with different batches of methylated ssDNA would be comparable.

In order to determine whether RecA influence demethylation activity of AlkB protein, reactions were performed at pH 8.0 by using purified RecA–AlkB complex (0.25 μM) or AlkB (0.25 μM) alone (Figure 4A) and oligo-N3me-C (1 μM) as substrate. Reactions were also carried out by RecA (1 μM) alone without any AlkB. As expected, AlkB demonstrated a moderate demethylation activity, whereas RecA alone did not produce any formaldehyde, indicating that it has no activity alone (Figure 4B). By contrast, a RecA and AlkB together exhibited very robust demethylation activity that was ∼2-fold stronger than AlkB alone (Figure 4C), indicating that RecA–AlkB complex is more efficient oxidative demethylase than AlkB alone.

We observed that at least 6-fold molar excess of RecA protein would have enough monomeric form to bind AlkB to form AlkB–RecA hetrodimer (Figure 2E). Therefore, demethylation reactions were performed with AlkB while separately adding RecA to the reaction mixture. Increasing amounts of RecA (0.87–28 μM) was added to fixed amount of AlkB (1 μM) keeping oligo-N3me-C substrate concentration constant (1 μM). As shown in Figure 4D, a gradual increase of formaldehyde release was observed until RecA molar concentration reached approximately seven to eight times higher than AlkB protein concentration; Increasing RecA concentration beyond this resulted only marginal increase in formaldehyde release (Figure 4D). From this result it appears that AlkB molecules are likely to bind free monomeric RecA protein that are available for interaction and the magnitude of stimulation of AlkB activity may depend on the concentration of the AlkB–RecA complex but not on the total RecA protein (Figure 4J). Hence, when all the AlkB protein was in complex with RecA, additional RecA protein had no effect on AlkB activity (Figure 4D).

We also assessed whether ATP hydrolysis by RecA further stimulates AlkB activity. As shown in Figure 4H and I, no additional increase of AlkB activity was observed when the repair reaction was performed with AlkB in the presence of RecA, $Mg^{2+}$ and a non-hydrolyzable ATP analog (ATP-γ-S). We next examined the effect of deletion of NTD of RecA on AlkB activity. Since NTD of RecA is essential for interaction with AlkB (Figure 3) and formation of nucleoprotein filaments on ssDNA (26), it was expected that addition of Δ33RecA to the repair reaction would have no effect on AlkB activity. We generated the Δ33RecA deletion mutant and purified the recombinant mutant protein (Figure 3C). As expected, addition of Δ33RecA (7 μM) to AlkB (1 μM) had a minimal effect on AlkB activity (Figure 4H and I). To establish whether RecA-mediated stimulation of DNA repair is directly linked to the Fe(II)-2OG-dependent dioxygenase activity of AlkB and not due to a fortuitous consequence of protein-DNA interaction, we used a catalytically-dead AlkB (His131Ala and His133Ala, Figure 4E) in the repair reaction (28). As shown in Figure 4F and G, mutant AlkB alone had very little activity and no increase in DNA repair was observed when RecA protein was added to the reaction. To check whether RecA-mediated stimulation is due to any stabilization effect, we performed AlkB repair reaction in the presence of BSA instead of RecA. As shown in Figure 4F and G, addition of BSA had no effect on the AlkB-mediated repair reaction. Together, these results confirm that catalytically-active AlkB is essential for RecA-mediated stimulation of ssDNA repair.

To further investigate RecA-mediated stimulation, we measured the demethylation reaction by increasing concentrations of AlkB (0.2–1.0 μM) or RecA–AlkB (0.14–7 μM) with 0.76 μM 40-mer N3-me oligo-dC. As shown in Supplementary Figure S3A, the demethylation rate increased linearly with AlkB concentration, which was an expected result. Interestingly, plot of the demethylation against AlkB–RecA concentration also showed linear increase, albeit with steeper gradient.

A simple model to explain the RecA-mediated stimulation of AlkB activity would be that the RecA increases the affinity of AlkB for methylated ssDNA. To address this, we analyzed AlkB activity under standard conditions using 40-mer N3-me oligo-dC as substrate and value of the Michaelis-Menten kinetic parameter ($K_M$ and $k_{cat}$), which gives an indication of the enzyme-substrate kinetics, was determined (Supplementary Figure S3B). The $K_M$ and $k_{cat}$ values we report here using 40-mer N3-me oligo-dC substrate are similar to that of a previously reported $K_M$ and $k_{cat}$ obtained with 19-mer oligo containing a single N3meC (29). Next, we checked AlkB activity in the absence and presence of RecA and observed that the apparent $K_M$ value stayed the same, 2.725 and 2.717 μM, respectively (Supplementary Figure S3B). These data confirm that interaction of RecA may not alter the intrinsic affinity AlkB for methylated DNA. Instead, kinetic analyses indicate that AlkB–RecA has higher activity ($K_{cat}/K_M = 1.051\ \mu M^{-1}\ s^{-1}$) than for AlkB ($K_{cat}/K_M = 0.695\ \mu M^{-1}s^{-1}$), suggesting that the stimulatory role of RecA may be more complex than simple alteration of substrate specificity. We have also examined if binding of a protein to ssDNA substrate would affect the ability of AlkB to carry out demethylation. We analyzed AlkB activity in presence of *E. coli* single-strand DNA binding protein (SSB) under standard conditions. As shown in Supplementary Figure S3B, presence of SSB did not change Michaelis-Menten kinetic parameters, suggesting that AlkB activity is not influenced by protein binding to the ssDNA substrate.

To investigate if the interaction of RecA with AlkB could impact RecA function, we analyzed the effect of loss of AlkB on cell survival after exposure to ultraviolet (UV) radiation, ionizing radiation (IR) and MMS. Deletion of the *recA* gene resulted small change in the survival to MMS (Supplementary Figure S5A). As expected, *alkB* and *alkB recA* strains showed similar sensitivity to MMS. The survival of the *alkB* mutants to UV was similar to wild-type (Supplementary Figure S5B) while the *recA* mutant and *recA alkB* double mutant were equally sensitive to UV. With IR, the results were similar; lack of AlkB had little effect on survival (Supplementary Figure S5C). In general, these results suggest that AlkB–RecA interaction may not influence RecA function.

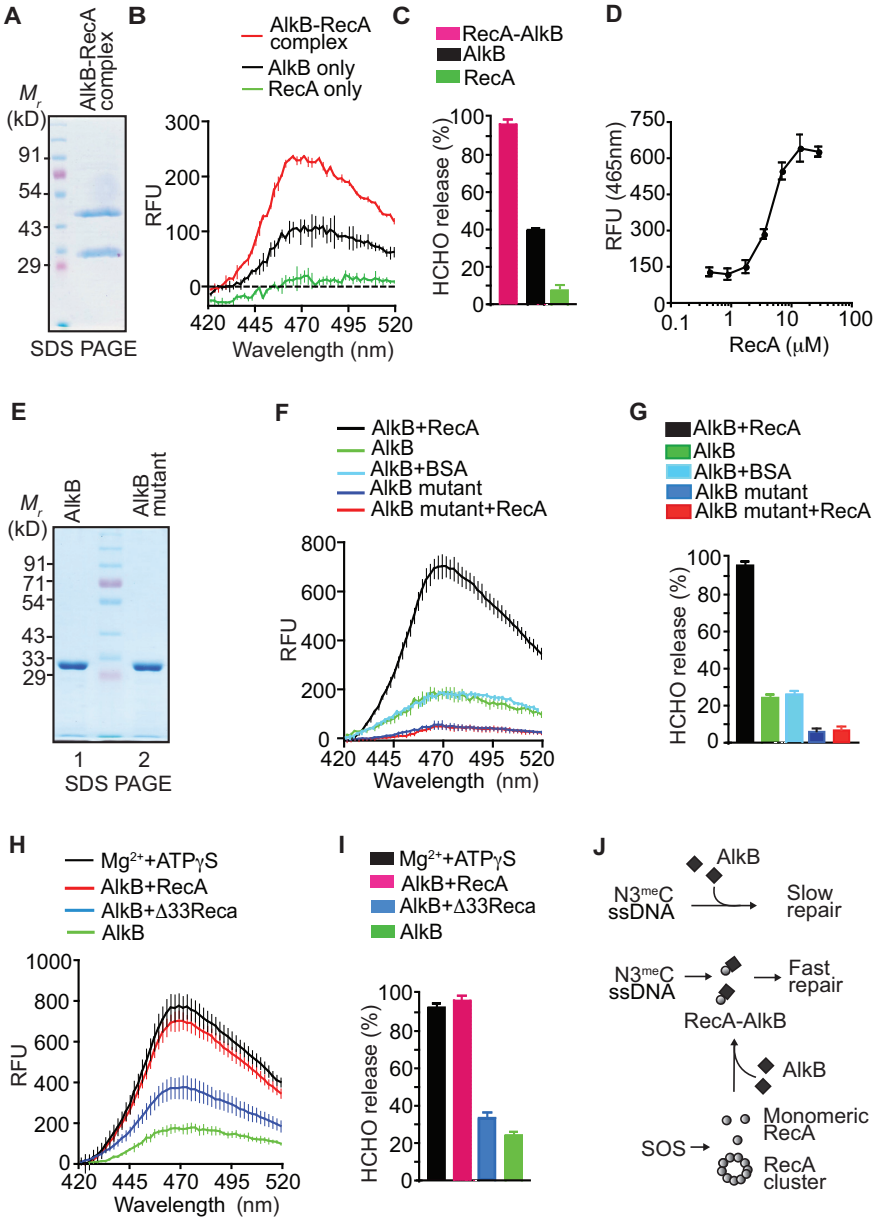


**Figure 4.** RecA enhances AlkB-mediated direct repair. (**A**) SDS-PAGE analysis of purified AlkB–RecA complex (**B**) Comparison of DNA repair by AlkB (0.25 μM) only or purified AlkB–RecA complex (0.25 μM) or RecA (1 μM) alone. About 1 μM 40-mer N3-meC oligo-dC was used as substrate in the presence of 20 mM Tris–HCl (pH 8.0). Fluorescence emission spectra of formaldehyde released during demethylation of 40-mer N3-me oligo-dC ($E_{max}$ 465 nm). Graphs represent averages of triplicate experiments. Dotted line depicts the zero value of the Y axis (**C**) Comparison of demethylation reactions represented in (B). Amount of released formaldehyde with RecA–AlkB was considered as 100% (**D**) DNA Repair with AlkB (1 μM) and increasing concentration of RecA (0.87–28 μM). (**E**) SDS-PAGE analysis of purified recombinant His-AlkB and catalytically dead mutant AlkB. (**F**) Demethylation reaction with mutant AlkB and BSA. Reaction included mutant AlkB (1 μM) and 40-mer N3-me oligo-dC DNA (1 μM) in presence of RecA or Δ33RecA. BSA (7 μM) was added instead of RecA (**G**) Comparison of demethylation reactions depicted in (E). Amount of released formaldehyde with RecA plus AlkB was considered as 100%. (**H**) The Effect of ATP and $MgCl_2$ on AlkB-mediated demethylation reaction. AlkB (1 μM), 40-mer N3-me oligo-dC DNA (1 μM) in the presence of 7 μM of RecA or Δ33RecA with or without $MgCl_2$ (1 mM) and ATP-γ-S (300 μM) (**I**) Comparison of demethylation reactions depicted in (H). Amount of released formaldehyde with RecA plus AlkB was considered as 100% (**J**) Schematic model RecA–AlkB complex formation. We conclude that majority of the RecA protein forms cluster in the absence of DNA or forms nucleoprotein filament in the presence of ssDNA. Only a small fraction of RecA exists as 'free' form and binds to AlkB. To obtain a 1:1 RecA–AlkB complex *in vitro*, 6 to 7-fold molar excess of RecA will be required. However, once RecA–AlkB complex is formed it makes a stable complex and promotes faster repair of alkylation adducts.

Our findings reported herein have revealed an unanticipated function of *E. coli* RecA, namely that it can augment repair of methylated ssDNA by AlkB. To our knowledge, this is the first study to identify a DNA repair function for RecA outside of its well-established role in recombinational DNA repair and part of DNA polV complex (21). Although most models of AlkB function propose that it acts alone in scanning the genome for damaged bases, we note that some reports are consistent and suggestive of a role for RecA in demethylation repair. For example, a *recA alkB* double mutant manifested a greater defect in reactivation of methylated M13 phage than an *alkB* single mutant, suggesting an additive effect of RecA (10). Production of large amount of RecA protein during SOS response may result AlkB–RecA complex with an improved catalytic power. Since RecA does not have any specificity for alkylation damage, the fundamental raison d'être for RecA–AlkB complex formation might be to enhance AlkB-mediated ssDNA repair. It will be of importance to determine whether more complex organisms have evolved a similar mechanism.

## SUPPLEMENTARY DATA

Supplementary Data are available at NAR Online.

## ACKNOWLEDGEMENTS

We thank Dr Luke A. Selth, Dame Roma Mitchell Cancer Research Laboratories and Adelaide Prostate Cancer Research Centre, The University of Adelaide, SA, Australia for editing the manuscript. We thank Dr N. Ganesh (Indian Institute of Science, Bangalore) and Dr K. Gopinath (University of Hyderabad, Hyderabad) for reagents and technical help.

## FUNDING

Department of Biotechnology (DBT); Ministry of Human Resource Development (MHRD), Govtvernment of India. *Conflict of interest statement.* None declared.

## REFERENCES

1. Shrivastav,N., Li,D. and Essigmann,J.M. (2010) Chemical biology of mutagenesis and DNA repair: cellular responses to DNA alkylation. *Carcinogenesis*, **31**, 59–70.
2. Blair,I.A. (2008) DNA adducts with lipid peroxidation products. *J. Biol. Chem.*, **283**, 15545–15549.
3. Winczura,A., Zdzalik,D. and Tudek,B. (2012) Damage of DNA and proteins by major lipid peroxidation products in genome stability. *Free Radic. Res.*, **46**, 442–459.
4. Fu,D., Calvo,J.A. and Samson,L.D. (2012) Balancing repair and tolerance of DNA damage caused by alkylating agents. *Nat. Rev. Cancer*, **12**, 104–120.
5. Falnes,P.O., Johansen,R.F. and Seeberg,E. (2002) AlkB-mediated oxidative demethylation reverses DNA damage in Escherichia coli. *Nature*, **419**, 178–182.
6. Trewick,S.C., Henshaw,T.F., Hausinger,R.P., Lindahl,T. and Sedgwick,B. (2002) Oxidative demethylation by Escherichia coli AlkB directly reverts DNA base damage. *Nature*, **419**, 174–178.
7. Kurowski,M.A., Bhagwat,A.S., Papaj,G. and Bujnicki,J.M. (2003) Phylogenomic identification of five new human homologs of the DNA repair enzyme AlkB. *BMC Genomics*, **4**, 48.
8. Begley,T.J. and Samson,L.D. (2003) AlkB mystery solved: oxidative demethylation of N1-methyladenine and N3-methylcytosine adducts by a direct reversal mechanism. *Trends Biochem. Sci.*, **28**, 2–5.
9. Delaney,J.C., Smeester,L., Wong,C., Frick,L.E., Taghizadeh,K., Wishnok,J.S., Drennan,C.L., Samson,L.D. and Essigmann,J.M. (2005) AlkB reverses etheno DNA lesions caused by lipid oxidation in vitro and in vivo. *Nat. Struct. Mol. Biol.*, **12**, 855–860.
10. Dinglay,S., Trewick,S.C., Lindahl,T. and Sedgwick,B. (2000) Defective processing of methylated single-stranded DNA by E. coli AlkB mutants. *Genes Dev.*, **14**, 2097–2105.
11. Holland,P.J. and Hollis,T. (2010) Structural and mutational analysis of Escherichia coli AlkB provides insight into substrate specificity and DNA damage searching. *PLoS One*, **5**, e8680.
12. Cox,M.M. (2007) Motoring along with the bacterial RecA protein. *Nat. Rev. Mol. Cell Biol.*, **8**, 127–138.
13. West,S.C., Cassuto,E. and Howard-Flanders,P. (1981) recA protein promotes homologous-pairing and strand-exchange reactions between duplex DNA molecules. *Proc. Natl. Acad. Sci. U.S.A.*, **78**, 2100–2104.
14. Story,R.M., Bishop,D.K., Kleckner,N. and Steitz,T.A. (1993) Structural relationship of bacterial RecA proteins to recombination proteins from bacteriophage T4 and yeast. *Science*, **259**, 1892–1896.
15. Story,R.M., Weber,I.T. and Steitz,T.A. (1992) The structure of the E. coli recA protein monomer and polymer. *Nature*, **355**, 318–325.
16. Story,R.M. and Steitz,T.A. (1992) Structure of the recA protein-ADP complex. *Nature*, **355**, 374–376.
17. VanLoock,M.S., Yu,X., Yang,S., Lai,A.L., Low,C., Campbell,M.J. and Egelman,E.H. (2003) ATP-mediated conformational changes in the RecA filament. *Structure*, **11**, 187–196.
18. Cox,M.M. (2007) Regulation of bacterial RecA protein function. *Crit. Rev. Biochem. Mol. Biol.*, **42**, 41–63.
19. Little,J.W. (1991) Mechanism of specific LexA cleavage: autodigestion and the role of RecA coprotease. *Biochimie*, **73**, 411–421.
20. Schlacher,K., Cox,M.M., Woodgate,R. and Goodman,M.F. (2006) RecA acts in trans to allow replication of damaged DNA by DNA polymerase V. *Nature*, **442**, 883–887.
21. Gruber,A.J., Erdem,A.L., Sabat,G., Karata,K., Jaszczur,M.M., Vo,D.D., Olsen,T.M., Woodgate,R., Goodman,M.F. and Cox,M.M. (2015) A RecA protein surface required for activation of DNA polymerase V. *PLoS Genet.*, **11**, e1005066.
22. Pierce,B.G., Wiehe,K., Hwang,H., Kim,B.H., Vreven,T. and Weng,Z. (2014) ZDOCK server: interactive docking prediction of protein-protein complexes and symmetric multimers. *Bioinformatics*, **30**, 1771–1773.
23. Kozakov,D., Beglov,D., Bohnuud,T., Mottarella,S.E., Xia,B., Hall,D.R. and Vajda,S. (2013) How good is automated protein docking? *Proteins*, **81**, 2159–2166.
24. Comeau,S.R., Gatchell,D.W., Vajda,S. and Camacho,C.J. (2004) ClusPro: a fully automated algorithm for protein-protein docking. *Nucleic Acids Res.*, **32**, W96–W99.
25. Brenner,S.L., Zlotnick,A. and Griffith,J.D. (1988) RecA protein self-assembly. Multiple discrete aggregation states. *J. Mol. Biol.*, **204**, 959–972.
26. Lee,C.D. and Wang,T.F. (2009) The N-terminal domain of Escherichia coli RecA have multiple functions in promoting homologous recombination. *J. Biomed. Sci.*, **16**, 1–13.
27. Shivange,G., Kodipelli,N., Monisha,M. and Anindya,R. (2014) A role for Saccharomyces cerevisiae Tpa1 protein in direct alkylation repair. *J. Biol. Chem.*, **289**, 35939–35952.
28. Westbye,M.P., Feyzi,E., Aas,P.A., Vagbo,C.B., Talstad,V.A., Kavli,B., Hagen,L., Sundheim,O., Akbari,M., Liabakk,N.B. *et al.* (2008) Human AlkB homolog 1 is a mitochondrial protein that demethylates 3-methylcytosine in DNA and RNA. *J. Biol. Chem.*, **283**, 25046–25056.
29. Roy,T.W. and Bhagwat,A.S. (2007) Kinetic studies of Escherichia coli AlkB using a new fluorescence-based assay for DNA demethylation. *Nucleic Acids Res.*, **35**, e147.